energies

IMPACT FACTOR 3.2

CITESCORE 7.3

Article

Editor's Choice

Offshore Wind Farm Economic Evaluation Under Uncertainty and Market Risk Mitigation

Antonio C. Caputo, Alessandro Federici, Pacifico M. Pelagagge and Paolo Salini

MDPI

https://doi.org/10.3390/en18092362

energies

MDPI

Article

Offshore Wind Farm Economic Evaluation Under Uncertainty and Market Risk Mitigation

Antonio C. Caputo [1,*], Alessandro Federici [2], Pacifico M. Pelagagge [2] and Paolo Salini [2]

[1] Department of Industrial, Electronic and Mechanical Engineering, University Roma Tre, Via Vito Volterra, 62, 00146 Roma, Italy
[2] Department of Industrial Engineering, Information and Economics, University of L'Aquila, Zona Industriale di Pile, 67100 L'Aquila, Italy; alessandro.federici@graduate.univaq.it (A.F.); pacifico.pelagagge@univaq.it (P.M.P.); paolo.salini@univaq.it (P.S.)
* Correspondence: acaputo@uniroma3.it

Abstract: Renewable energy systems (RES) are strongly affected by many sources of uncertainty and variability. Nevertheless, traditional technical and economic evaluation methods often neglect uncertainty by deterministically assuming average nominal values, using simple sensitivity analysis to explore effects of changing conditions, or limiting to a few sources of uncertainty. Furthermore, long-term variability and changing scenarios during the life of the system are not considered. This leads to inaccurate estimation of inherent investment risk. To address this gap, this work proposes a framework for the economic evaluation of offshore wind farms, considering the effects of both epistemic and aleatory uncertainty. Uncertainty of correlations used to model the system, the variability of resources and energy prices, as well as the use of a financial hedging tool to cope with market risk, the impact of failures and disruptive events, the changing of long-term scenarios during the system's life, and the wake effect due to wind direction variability are all considered. As demonstrated through an example of an application, this methodology will be useful to practitioners and academics to achieve a more realistic assessment of the profitability of the investment based on a more comprehensive propagation of uncertainty.

Keywords: offshore wind power system; economic evaluation; risk analysis; uncertainty propagation

check for updates

Academic Editor: Davide Astolfi

Received: 14 February 2025
Revised: 25 April 2025
Accepted: 29 April 2025
Published: 6 May 2025

Citation: Caputo, A.C.; Federici, A.; Pelagagge, P.M.; Salini, P. Offshore Wind Farm Economic Evaluation Under Uncertainty and Market Risk Mitigation. *Energies* **2025**, *18*, 2362. https://doi.org/10.3390/en18092362

1. Introduction

Wind power generation is a widespread technology playing a relevant role in the world decarbonization strategy. Although the current capacity growth is still dominated by onshore plants, offshore installations are progressively increasing their share, being in the early stage of expansion. The entire sector has been characterized by a huge growth in investments in recent years, and it has been forecasted that this investment will continue to increase in the near future [1]. However, other economic observers, such as McKinsey & Co. consulting firm, warn that after a decade of strong value creation, the offshore wind industry may be at a turning point, as recent macroeconomic trends (rising raw commodity prices, interest rate hikes, and supply chain bottlenecks) have put pressure on offshore wind developers' profitability [2]. They identify five profit drivers, namely material cost fluctuations, regulatory landscape, strength of market pull, supply chain stability, and developer behavior, highlighting the importance of scenario analysis to counter current levels of uncertainty.

Wind energy reduces both the dependence on fossil fuel and greenhouse gas emissions. Wind power is theoretically limitless and avoids the release of harmful pollutants. In addition, since wind power is available at the site of installation of the system, it increases the energy security of a country while decreasing the price fluctuation associated with fossil fuel imports. Another important advantage of this technology is its scalability. Its applications range from residential uses to large-scale wind farms, both onshore and offshore. Passing from a single wind turbine to a wind farm offers significant advantages in terms of economy of scale, thus reducing the overall Levelized Cost of Electricity.

While onshore wind energy conversion technology can be considered mature, offshore wind power systems are still considered an evolving technology, with ongoing exploration of novel technical solutions. One of the key advantages of offshore wind power is the absence of land consumption and the lack of obstacles to wind flow, providing significant benefits over land-based wind turbines. Additionally, the reduced visual impact of offshore wind farms leads to better public acceptance. However, it is important to note that offshore wind farms face higher installation and operational costs compared to their onshore counterparts. These costs are primarily attributed to logistical challenges, the demanding operational environment, and the increased distance from users. Moreover, installation in increasingly deep waters substantially increases mooring and deployment costs, also requiring new architectural solutions for the floating platforms.

However, as is the case with most renewable energy conversion systems (RES), even wind power suffers from the high variability of the sources, which are not available on demand. Furthermore, while theoretically there is no limit to site location, some geographic areas may be unsuitable for the installation of offshore wind power systems. Apart from site-specific constraints related to marine life preservation, other infrastructures presence, or national zoning issues, the risk of investment increases, making it non-economically viable; if the mean wind speed is not sufficiently high, or when its standard deviation is too large. In Europe, for instance, this penalizes installations in the Mediterranean Sea as compared with those in the northern seas, owing to lower average wind speed and greater average sea depth, necessitating floating installation with higher mooring costs. In addition, RES have to deal with traditional sources of uncertainty, such as equipment failures and market price variability. In this complex environment, more dependable techniques for the economic assessment of RES investments must be developed to ensure accurate risk estimation. The presence of various sources of uncertainty in wind farms, both epistemic (stemming from a lack of knowledge but theoretically reducible) and aleatory (arising from random phenomena and inherently irreducible), significantly impacts the profitability of such investments, thereby increasing investment and financial risks [3]. Inaccurate risk assessment can lead to erroneous decisions, resulting in incorrect designs and poor profitability. Effective risk mitigation strategies, including financing instruments, play a crucial role in managing these risks [4]. Their incorporation during the design, planning, and assessment phases is vital to mitigate potential adverse effects.

In wind power systems evaluation methods, uncertainties typically encompass imprecise turbine design relationships, wind speed variability, and the sales price of generated energy. However, uncertainties arising from downtime and costs resulting from random failures of internal components [5–7], as well as disruptive external events stemming from natural hazards and man-made incidents (such as ship collisions, rogue waves, earthquakes, etc.), which pose a significant risk of system destruction and premature termination of its useful life, are often overlooked or neglected.

Numerous papers in the literature focus only on specific sources of uncertainty in wind power systems. For instance, some studies concentrate solely on the aleatoric uncertainty of wind speed [8–11] or combine it with the uncertainty of energy price forecasting [12].

Others include additional factors such as the epistemic uncertainty of wind power forecasting [13], power curve [14], manufacturing tolerances, and insect contamination [15], as well as the wake effect and unavailability of wind turbines [16]. A recent study [17] concurrently considers the uncertainties of wind speed, energy price, and power curve. The five most relevant investment risk types in renewable energy technology are curtailment, policy, price, resource, and technology and several qualitative drivers lead their change over time [18], as pointed out by a qualitative research reporting expert opinions. Recently, a system dynamics method for risk evaluation for onshore and offshore wind power has been introduced [19]. This method established qualitative interrelationships between the key factors of the investment risk and allowed for simulation of the investment risk trend over a long-time period. The selected risk drivers are the same as in the previously mentioned study. Very often, risk sources and levels in this field are estimated resorting to experts' opinions. In the literature, these judgments have been used to propose an integrated model for risk evaluation and cost estimation [20]. In that contribution, the risks are identified using a systematic literature review, then the first step of risk analysis is conducted with modified fuzzy group decision-making and, finally, the risk analysis is concluded resorting to Monte Carlo simulation methods relying on aggregate uncertain variables such as investment cost, operational cost, produced energy, and revenues. Insurances, financial derivatives, and diversification are only three examples of the existing strategies for risk management and mitigation both for onshore and offshore wind parks [21]. In this respect, an advanced approach to risk analysis of onshore wind energy investment has been proposed in the past years using real options theory combined with Monte Carlo simulation [22]. Even if the authors do not include some relevant uncertainty sources, they demonstrate that traditional techniques that do not consider uncertainty and the relative compensation, resorting to flexibilities during the design phase, could lead to non-cost-effective investments. Lei et al. [23] considered few sources of uncertainty but proposed a method to maximize the net present value and the discount rate while minimizing the payback time. As far as wind farms are concerned, the literature includes a review of methodological approaches for their design and optimization [24]. This work presents state-of-the-art models and real-world applications of wind farm optimization strategies. Additionally, economic assessment studies on offshore wind energy systems have been reviewed, including a recent contribution that analyses the economic and technical feasibility indicators of offshore wind farms [25]. However. In this review work nonspecific quantitative model is developed and the uncertainty issue is neglected.

Yilmazlar et al. [26], for instance, use a dynamic cost model to adjust capital investment to market conditions and utilize it to determine the optimal wind farm layout considering wind variability in the Sardinia region. Borràs Mora et al. [27] modify the deterministic OWCAT cost estimation model to account for variability and uncertainty in offshore wind farms modeling. They mainly model uncertainty resorting to probability density function of uncertain variables, thus focusing on Type II uncertainty according to the classification used in this paper and mainly consider cost items and financial parameters. Borràs Mora et al. [28] explore the impact of wind speed uncertainty on debt project financing issues. Borràs Mora et al. [29] perform a global sensitivity analysis to identify relevant contributors to offshore wind farms economics uncertainty mainly focusing on average wind speed variability and the various components of investment and installation costs. Ioannou et al. [30] use Monte Carlo analysis to assess the impact of capital investment and operating expenses on wind farm levelized energy cost. Other authors focus on operations and maintenance uncertainties. Rinaldi et al. [31] examine the impact of operations and maintenance costs of wind farms on produced electricity cost variability, while Dinwoodie et al. [32] examine alternative operational strategies of wind farms accounting for random failures.

The above review points out that earlier literature only focuses on one or a few sources of uncertainty at a time, often uses qualitative modeling, neglects future scenario variations and mostly considers uncertain variables amenable to a characterization through a predetermined probability distribution only, neglecting other variability types such as discrete disruptive events and temporal discontinuities.

However, despite discussions by [33,34] that highlight the absence of an all-encompassing model incorporating and integrating all sources of variability, a recent paper by Caputo et al. [35] proposes a framework for evaluating wind power systems under uncertainty, considering both epistemic and aleatory uncertainty, component failures, and disruptive events. Nonetheless, that study is limited to a single wind turbine. Furthermore, long-term variability and scenario variations throughout the system's lifespan are not taken into account.

Many computer tools have been developed for analyzing the integration of renewable energy into several energy systems, but they are often limited to a single energy source, a single region, or are specific to some objective [36]. Moreover, the currently available commercial software tools for the economic assessment of wind power systems typically rely on deterministic sensitivity analysis, where variables values are modified one at a time [37]. Even the tools that incorporate variability [38] only consider a limited number of uncertainty sources. Others [39] overlook important factors such as component efficiencies and further significant sources of uncertainty. Similarly, SAM [40] fails to incorporate random events and component failures, as discussed in the review by Caputo et al., 2023 [35].

As a consequence, despite numerous attempts have been made to account for uncertainty and variability wind energy systems, an all-encompassing, integrated model for risk assessment on offshore wind farms is not available yet. In this paper, to cope with this literature gap, a comprehensive method for investment risk assessment of industrial plants is applied to offshore wind farms case. This approach is not limited to the evaluation of current investment but also includes future scenarios analysis for planning delayed investment. The correct planning of the date to invest in high-risk investments, such as offshore wind farms located in geographic areas characterized by a relatively low level of wind speed, is crucial. Indeed, nowadays, even countries with relatively mild wind conditions, e.g., Italy, are interested in investing in renewable energy to achieve the goals of decarbonization plans.

The proposed methodology comprehensively considers the key sources of epistemic and aleatory uncertainty, enabling more accurate estimation of the associated investment risk. By incorporating these uncertainties, this approach provides valuable support to practitioners, managers, and academics in the decision-making process. The novelty of this work can be attributed to three distinct aspects. Firstly, to the best of our knowledge, there is a noticeable absence of papers specifically focused on the economic evaluation of offshore wind farms under uncertainty. While the work of Caputo et al. [35] includes the main sources of uncertainty, it is limited to analyzing a single wind turbine, thereby neglecting crucial factors such as scale economies and the wake effect resulting from wind direction and interactions between wind turbines. In the second place, this research introduces a novel aspect by incorporating the changing long-term scenarios during the system's lifespan into the evaluation framework. This addition considers a previously overlooked source of uncertainties, providing a more comprehensive analysis. Lastly, a market risk mitigation tool resorting to financial tools is introduced for the first time within the framework, allowing for a more accurate estimation of the profitability of wind farms. This integration marks a significant advancement in the field, enhancing the understanding of the associated risks and enabling more informed decision-making. In addition, since this new model includes future scenarios about the investment cost reduction due to learning effect and long-term variability of electricity and subsidies policy, it is able to evaluate high-risk investment that will occur in geographic areas characterized by a relatively low wind speed but potentially relevant in the future to achieve decarbonization goals.

In summary, the novel contribution of this study, in comparison to the earlier literature, can be itemized as follows:

- An overarching integrated, flexible, and modular framework freely extensible to include a wide and increasing range of uncertain factors and risk sources is developed.
- Multiple sources of uncertainty, often modeled individually and in a mutually exclusive manner, are concurrently considered.
- Multiple types of uncertainty sources are concurrently analyzed, namely random fluctuations of variables over time, occurrence of random values according to a predefined probability density function, occurrence of unpredictable discrete events of varying intensity, and random discontinuities determining changes in scenarios.
- Long term variability issues are included based on an articulated quantitative multiple scenario analysis, instead of resorting to simple best case/worst case analysis.
- Adoption of financial hedging tools is included in the economic assessment of investment.

The paper is structured as follows. Firstly, the approach to evaluate the technical and economic performance of wind farms is introduced, extending the existing model proposed in [35], accounting for the wake effect considering the wind direction and wind farm geometry. Subsequently, an overall framework for accounting uncertainty effects is described including the utilization of financial derivatives to mitigate market risk. Furthermore, the incorporation of changing long-term scenarios and the associated uncertainty is discussed. Finally, a case study is presented to demonstrate the model's capabilities, referring to a wind farm located in the Adriatic Sea, where average wind speed is low compared to more favorable areas for wind power exploitation. The paper concludes with a discussion of the model's limitations and perspectives for future research.

2. Framework for Offshore Wind Farms Economic Evaluation Under Uncertainty

The proposed framework for the economic evaluation of offshore wind farms (Figure 1) is an extension of the general framework proposed in Caputo et al. [35] and adopts a modular structure that allows for the user-defined activation of specific modeling blocks to address various sources of uncertainty. As compared to that earlier contribution, the novel features of this model are namely: (a) the extension from a single offshore turbine to a wind farm, including economies of scale and consideration for wake effects; (b) inclusion of long-term variability effects resorting to a systematic procedure for future scenarios generation in order to account for market and geopolitical risk (affecting energy price), regulatory risk (subsidies policy), and investment risk (related to learning effects based on trends of installed capacity base); (c) inclusion of financial hedging tool to mitigate profitability risk.

At its core, the model utilizes a Monte Carlo analysis method, which involves simulating a series of random occurrences of the system's lifespan over a predetermined number of iterations.

In the subsections below, the system model blocks will be briefly described.

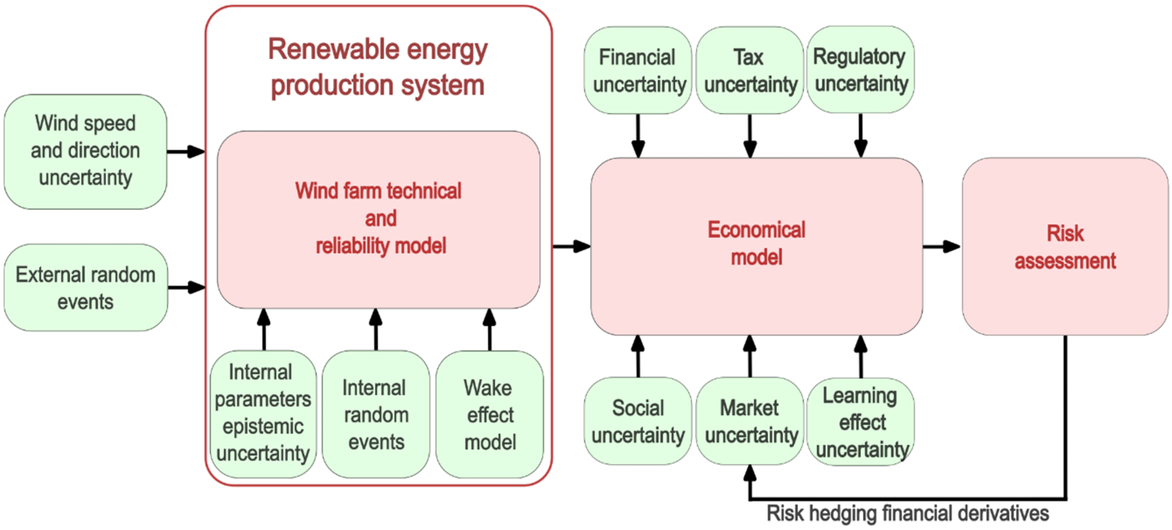

Figure 1. Proposed general framework for economic performance evaluation of renewable energy system.

2.1. Technical and Reliability Model

Using a technical model, based on Mathew's work [41], we can calculate the power output (P, in MW Equation (1)) of a horizontal axis wind turbine from real-time wind speed. This calculation is crucial for determining energy sales revenue and, consequently, the profitability of wind turbine investments.

$$P = \frac{1}{2} c_p \rho S U^3 \eta_g \eta_{gb} \eta_{pe} \cdot 10^{-6} \quad (1)$$

The extracted power P is calculated using the following parameters: undisturbed wind speed (U), rotor swept area (S), air density (ρ), turbine-specific power coefficient (c_p) [41], gearbox efficiency (η_{gb}), generator efficiency (η_g), and power electronics efficiency (η_{pe}). As discussed in Section 2.3.3, the power coefficient and efficiency values are subject to epistemic uncertainty, while wind speed (U) exhibits aleatory uncertainty (Section 2.3.1). Component failures significantly impact wind turbine availability and power output. To model these outages, an hourly availability array (A_{yh}) is generated (Section 2.3.4). This array contains a sequence of 0 s (turbine down) and 1 s (turbine operational) for each hour of the turbine's lifespan. The time series of wind speeds is instead stored in an hourly wind speed array (WS_{yh}). Using the turbine's power curve, this array is converted into the Nominal Produced Power array (NPP_{yh}). The actual hourly produced energy array is then calculated by element-wise multiplication of NPP_{yh} and A_{yh}.

$$HP_{yh} = NPP_{yh}(\cdot)A_{yh} \quad (2)$$

Calculating energy production becomes more complex when dealing with wind farms compared to single turbines, primarily due to the "wake effect". This effect causes a reduction in power output for turbines positioned downstream of others [42]. Specifically, as wind passes through the initial row of turbines, energy extraction and blade turbulence disrupt the flow, leading to a weaker, disturbed downstream wind pattern. Consequently, downstream turbines generate significantly less power than those upwind. This power deficit persists throughout the wind farm, potentially reaching 20% to 40% in large-scale installations [43], resulting in annual energy production losses of up to 15% [44]. Furthermore, the turbulence induced by rotors increases mechanical stress on downstream turbines, impacting both productivity, economic viability, and lifespan [45].

To mitigate the wake effect, wind farm layout optimization is crucial [46]. While various approaches exist to model wake effects [47] and ongoing research aims to quantify wake losses [48], this study utilizes Jensen's wake model [49,50]. This model is favored for its simplicity and relatively high accuracy in layout optimization studies [51] compared to other common wake models.

Jensen's model [50] calculates the wind speed deficit between upstream and downstream turbines (ΔU [m/s]) using the following parameters: undisturbed wind speed at the upwind turbine (U_a [m/s]) thrust coefficient (C_t) (which is wind speed dependent), horizontal distance between turbines (X_{ab} [m]), a wake decay constant (k), rotor swept area (A_b [m^2]), upwind turbine diameter (D_a [m]), and overlapped area between turbines (A_{ab} [m^2]).

$$\Delta U = U_a\left(1-\sqrt{1-C_t}\right)\left(\frac{D_a}{D_a+2kX_{ab}}\right)^2\frac{A_{ab}}{A_b} \tag{3}$$

When the distance (d) between the rotor centers of two wind turbines, projected onto a plane perpendicular to the wind direction, falls within the range of $0 < d < D_a$ (where D_a is the turbine diameter), the overlapped area (A_{ab}) can be calculated using Equation (4). The distance (d) itself is determined by Equation (5), utilizing the coordinates (x_a, y_a) and (x_b, y_b) of the rotor centers on the plane perpendicular to the wind direction. Intermediate values x and y, needed for Equation (4), are computed using Equations (6) and (7), respectively, where R_a and R_b represent the radii of the two wind turbines:

$$A_{ab} = R_a^2\sin^{-1}\left(\frac{y}{R_a}\right) + R_b^2\sin^{-1}\left(\frac{y}{R_b}\right) - y(x+\sqrt{R_b^2-R_a^2+x^2}) \tag{4}$$

$$d = \sqrt{(x_b-x_a)^2-(y_b-y_a)^2} \tag{5}$$

$$x = \frac{R_a^2-R_b^2+d^2}{2d} \tag{6}$$

$$y = \sqrt{R_a^2-x^2} \tag{7}$$

If the rotor centers of two turbines, projected onto a plane perpendicular to the wind direction, coincide (distance = 0), the overlapped area equals the rotor swept area. Conversely, if the distance between these centers exceeds the turbine diameter, the overlapped area is zero.

Because wind turbine rotors dynamically adjust the direction of their axis to maximize energy capture, the interaction between upwind and downwind turbines is not static. The overlapped area, and consequently the area overlap ratio, varies from 0 to the rotor swept area (A_b), and from 0 to 1, respectively, causing the wind speed deficit to fluctuate. Accurate determination of the overlapped area thus requires knowledge of wind direction and wind farm layout.

This implies that specific wind farm configurations can minimize wake losses. However, a trade-off exists between space utilization (affecting cabling and maintenance costs) and turbine spacing (aimed at reducing wake effects). Generally, as indicated in [52,53], a safe downstream spacing is 7–10 times the turbine blade diameter, while orthogonal spacing is typically 3–5 times the diameter.

The power computation process begins with acquiring accurate wind direction time series data. These data can be directly obtained or derived from x-axis and y-axis wind speed components. To capture wind direction variability, Monte Carlo sampling using a Kernel distribution [54] is employed, enabling a better fit to experimental data that may not conform to standard parametric density functions. Experimental data are fitted using the conditional probability of wind direction and wind speed, meaning that a given direction is considered relevant provided it is associated with a significant wind speed along that direction, thus ensuring realistic modeling.

The subsequent steps are:

1. Input Turbine Coordinates: Provide the coordinates of each turbine within the wind farm.
2. Calculate Distance Matrix: Compute the distance matrix (X_{ab}) between all turbine pairs.
3. Rotate for Wind Alignment: For each wind direction, rotate the system to align orthogonally.
4. Evaluate Overlapped Area Matrices: Calculate the overlapped area matrix (A_{ab}) for each turbine, accounting for potential influence from multiple turbines. Each entry of the matrix represents impact on turbine a by each b-th other turbine.
5. Compute Hourly Power: Using hourly wind speeds and corresponding overlapped areas, calculate the power generated by each turbine, resulting in a set of matrices representing hourly power output throughout the year.
6. Integration with Turbine Availability: Finally, the calculated power data are integrated with each turbine's up-time and down-time array [35].

Unlike the previous model, this approach recognizes that each turbine has a unique failure history and energy production record, contributing individually to the overall revenue.

2.2. Economical Model

The economic model calculates both costs and revenues, as detailed in [35]. The cost calculation considers the items listed in Table 1. The specific cost model used is thoroughly described in [55]. For estimating the floating platform costs, the methodology from [56] is used, and for installation procedures, ref. [57] is referenced. Corrective maintenance costs and revenue calculations are performed according to the methods in [35], adapted to account for the presence of multiple turbines.

Table 1. Cost model items.

Cost Item	Sub-Items	Literature Source
Investment cost	Wind turbine and floating platform purchase (wind turbine, floating platform, cables and transmission system, mooring and anchoring systems)	[55–57]
	Wind turbine and floating platform installation (loading onto vessel, sea transport, mooring, electrical cable lying, onshore cable installation) and rent of the shipyard	
Operating cost	Grid access fees, insurance costs, and seabed rental	
	Maintenance cost (preventive)	
	Maintenance cost (corrective)	[35]

When analyzing a wind farm, the cost of array cables significantly increases with the number of turbines and their geographical dispersion, and it represents a substantial portion of the overall investment. Optimizing wind farm layout involves balancing turbine spacing (to minimize wake effects) and space utilization (which impacts cable and transmission system costs). The farm layout also influences operational costs.

The annual failure list, generated using the methodology in [35], allows for the calculation of annual corrective maintenance costs. This calculation includes the cost of each individual failure, denoted as $\mathrm{ReC_i}$ (Equation (8)). Material costs are also incorporated, based on data from Carroll et al. [7].

$$ReC_i = C_t N_t RT_i + RC_i \quad (8)$$

The hourly cost of technicians is represented by C_t; RT_i is the recovery time for a failure; Nt is the number of technicians required for repair; and RC_i is the cost of materials used in the repair.

The annual revenue (R_y) for year y is calculated by element-wise multiplying the hourly produced electricity vector (HP_{yh}) with the hourly electricity price vector (EP_{yh}) and then summing the resulting values over all hours in the year (Equation (9)).

$$R_y = \sum_{h=0}^{8760} HP_{yh}(\cdot)EP_{yh} \tag{9}$$

In this equation, h represents a specific hour, and EP_{yh} denotes the simulated hourly electricity price vector.

2.3. Uncertainty Modeling

For a proper risk assessment, the above intrinsically deterministic model for technical and economic performances estimation must be fed with uncertain values of the involved variables and parameters. In addition to the commonly accepted classifications of uncertainty, such as endogenous (uncertainty that arises within the system) versus exogenous (uncertainty originating from outside the system), or epistemic (theoretically reducible uncertainty) versus aleatory (non-theoretically reducible), the perspective on the nature of uncertainty adopted in this work is based on the time trend of uncertain parameters. This classification directly lends itself to a risk assessment based on the life cycle of the system under study, i.e., its evolution over time, and directly helps in the choice of the proper uncertainty modeling approach. Four variability classes are considered as follows (Figure 2):

- Type I variability refers to the random fluctuations of variables over time. This behavior can be effectively modeled using techniques such as time series analysis and random processes. For example, in the context of wind power systems, Type I variability can be observed in the changing wind speed and direction over time or the fluctuation of electricity sales prices.
- Type II variability pertains to variables that assume a constant but unknown value, which can be described using a predefined probability density function. This type of uncertainty for instance is represented by uncertainty about the applicable interest rate or the efficiency of a conversion system.
- Type III variability involves the occurrence of unpredictable, discrete events of varying intensity. These events, such as equipment failures or natural disasters, can significantly disrupt system operations. Random process modeling is used to represent this type of uncertainty.
- Type IV variability consists of random discontinuities, where variables abruptly and unpredictably change values at unknown times. This uncertainty is often linked to fluctuations in economic, political, or regulatory environments throughout a system's lifespan.

Table 2 presents a summary of the sources of uncertainty included in this model and their corresponding classifications. The table indicates the affected variable, its variability type, the nature of uncertainty (epistemic, E, or aleatory, A), as well as the adopted modeling approach. All variables already included in [35] are dealt with, while the latter five items in the Table are additional novel sources of uncertainty that have been incorporated into this new model.

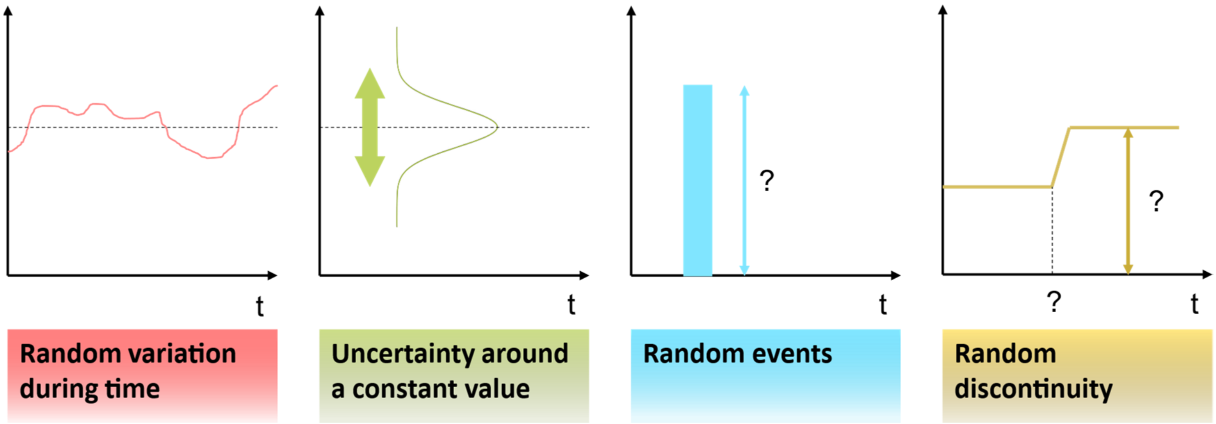

Figure 2. Uncertainty type classification ("?" symbol means an unknown value in the intensity level or time of occurrence).

Table 2. Considered sources of uncertainties.

Variable	Uncertainty Nature	Variability Type	Modeling Approach
Bank interest rate	E	II	Monte Carlo sampling from predefined pdf
Investment cost	E	II	
Plant nominal life	E	II	
Self-interest rate	E	II	
Power coefficient	E	II	
Gear box efficiency	E	II	
Generator efficiency curve	E	II	Monte Carlo sampling from predefined pdf centered on the nominal performance curve
Power electronic efficiency curve	E	II	
Number of required technicians for system restoring	E	II	
Repair costs	E	II	
Disruptive external events	A	III	Monte Carlo sampling from hazard curve and random generation of failure severity level from fragility curve
Components failures	A	III	Monte Carlo sampling of Time to failure pdf and Monte Carlo sampling of time to repair pdf
Wind speed	A	I	Markov chain
Electricity price	A	I	ARIMA time series
Wind direction	A	I	Monte Carlo sampling from predefined pdf
Wake effect	E	II	
Regulatory risk	A	IV	Scenario analysis
Long-term market risk	A	IV	
Investment cost-related risk	A	IV	

2.3.1. Wind Uncertainty Modeling

While the literature commonly relies on sampling Weibull probability distributions based on historical data to address this uncertainty [58–60], this approach can result in unrealistic sudden changes in speed and direction values. To mitigate this issue, this work adopts a Markov chain method, following the approach outlined by Negra et al. [61], to generate hourly time series of wind speeds over the entire lifespan of the plant. This methodology relies on the historical hourly wind speed record at the selected site. Given that available weather data refer to wind speed at 10 m above sea level, to assess the wind speed values at the height of the turbine's hub the log law is used [62]. In greater detail, the adopted method sets up a birth-and-death Markov process using the historical time series to calculate the number of possible states and the transition rates of the Markov process. The calculation of the number of possible states and the transition rates are strictly related to the maximum and minimum values of wind speed of the training time series and the time of permanence in certain states, respectively. This approach allows to consider both statistical parameters of the past values of wind speed and its randomness, generating a time-series of wind speed values for each run, to be stored in the hourly wind speed array WS_{yh}. The number of possible states and the transition rates depend on the maximum and minimum values.

2.3.2. External Random Events

External disruptive random events, such as terrorist acts, collisions with ships, earthquakes, and rogue waves, are modeled following the approach outlined by Huang et al. [63]. To assess the impact of these events, a library of fragility curves and expected damage can be constructed for each event type, either by developing them specifically or by drawing from the existing literature [64–68]. The generation of a list of disruptive event dates, magnitudes, and expected damage follows the methodology described in Caputo et al. [35].

2.3.3. Epistemic Uncertainty of Internal Parameters

In this model, epistemic uncertainty related to internal parameters stems from component efficiencies and model simplifications. To address this, probability density functions centered on mean values and bound by maximum and minimum values are used. Specifically, the technical model's epistemic uncertainty sources are the power coefficient, gearbox efficiency, generator efficiency curve, and power electronics efficiency curve. The chosen wake effect model, Jensen's model, also exhibits epistemic uncertainty, even in single wake scenarios, as documented in [69]. While Jensen's model is considered highly accurate at the wake center, particularly for wind speeds below 8.5 m/s, it tends to underestimate wake losses by 2–5% and overestimate wind speed reduction across the entire wake cone. The largest discrepancies between predicted and measured wind speeds occur at shorter distances. For downstream distances of 2.55 to 3.75 turbine diameters, measured average wind speeds are 12–14% higher than predicted. This error decreases to 7–12% at distances of 5.1 to 7.3 diameters. Despite the conservative nature of this underestimation, this model aims to reflect the system's actual uncertainty. Therefore, the wind speed value calculated by Jensen's model after wake decay is adjusted by sampling a value from a uniform distribution ranging from 0.07 to 0.12.

2.3.4. Internal Random Events

The wind turbine system is subdivided into components and subassemblies, following the approach presented in Tavner [70]. These components are considered to be in series, meaning that when a single element fails, the entire system fails, and production ceases until the component is repaired. To generate a time stamped list of failure events throughout the system's lifespan, the Monte Carlo technique is employed by sequentially sampling the distributions of the mean time between failures and mean time to repair for each component and subassembly based on the methodology described in [35]. Simulation of a failure's time history allows to determine the time trend of the instantaneous availability of each turbine, which can be paired with the concurrent wind speed time history. For each failure, the number of technicians and expected restoration costs are also sampled from the corresponding distributions to determine maintenance cost.

2.3.5. Economic Model Uncertainty

This section addresses uncertainties influencing economic and financial parameters, including electricity price fluctuations, capital investment uncertainty (incorporating learning effects and tax policies), and epistemic uncertainty in the economic model (bank interest rate, investment cost, plant lifespan, and self-interest rate). Investment cost calculations introduce epistemic uncertainty due to the underlying relationships. To account for this, the adopted values are sampled from a probability distribution based on the calculated expected value. Revenue calculation involves multiplying hourly power production by hourly energy prices, excluding downtime. Market risk is primarily modeled through hourly energy prices. Historical time series data are used for regression analysis, yielding coefficients for an autoregressive integrated moving average (ARIMA) model. Monte Carlo simulation generates 1000 price paths per run, and the median time series is used for revenue calculation in each run. Long-term variability is incorporated by using forecasted mean electricity price scenarios to define the time series' mean. The ARIMA model's coefficients vary based on the input data. For illustrative purposes, Equation (10) shows the structure of the adopted ARIMA (1,1,1) model:

$$y_y = (1 - \phi_1)m + (1 + \phi_1)y_{t-1} - \phi_1 y_{t-2} + e_t + \theta_1 e_{t-1} \tag{10}$$

In Equation (10), y represents the variable being regressed; θ_1 is the moving average coefficient; Φ_1 is the autoregressive coefficient; m is the drift term; e is the error term; and the subscript t indicates the time period.

To account for financial risk, Monte Carlo sampling is used, drawing values from predefined probability density functions for the plant's nominal lifespan, bank investment cost, and self-interest rate.

2.3.6. Long-Term Scenario Effects (Type IV Uncertainty)

To our knowledge, prior studies have not addressed Type IV uncertainty, which encompasses unpredictable discontinuities resulting from economic, political, and regulatory shifts, in conjunction with the other uncertainty sources. This omission limits the accuracy of long-term economic viability assessments. This work explicitly models scenario effects by incorporating long-term trends in average electricity prices, the impact of learning effects on capital investment, and changes in subsidy policies.

Specifically, market risk is modeled to capture both short-term energy price fluctuations and long-term changes across different scenarios. When evaluating future wind farm investments, it is also crucial to consider the potential for reduced investment costs due to the learning rate, termed 'investment cost-related risk' in Table 2. Furthermore, given the significant role of subsidies in the wind energy sector, potential long-term policy changes must be modeled, referred to as 'regulatory risk' in Table 2.

The model integrates investment cost reduction using the offshore wind power learning rate, as reported by Fortes et al. and Shields et al. [71,72], who estimate a constant learning rate of approximately 9%. This rate is combined with scenarios for projected European offshore wind power installed capacity by 2030 by Nghiem and Pineda [1]. Figure 3 illustrates the resulting learning effect curve, showing the price per installed megawatt as a function of the installation year, considering cumulative installed capacity growth.

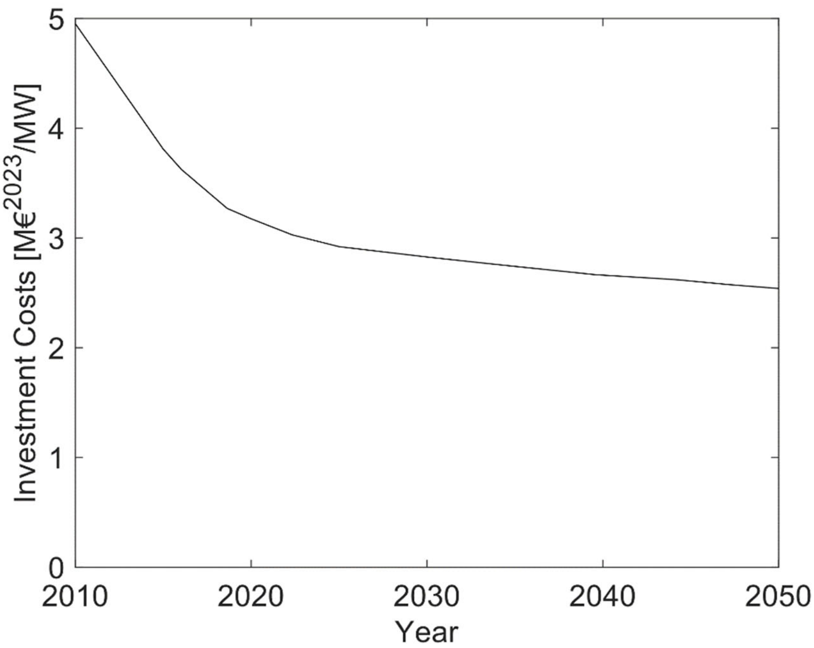

Figure 3. Learning rate-based decay of offshore wind power investment costs per MW over time.

To model long-term market and regulatory risks, commonly referenced scenarios from the existing literature are used [73], reporting on potential mean electricity prices and volatility trends. Short-term energy price variability is then simulated based on the expected yearly energy price from the chosen scenarios. Regulatory risk is modeled by considering different subsidy policies, such as no-subsidies, feed-in tariffs (fixed price), and feed-in premium tariffs (market price plus subsidy).

If scenarios affect multiple variables (e.g., electricity price, investment cost reduction, subsidies) and are not mutually exclusive, they can be combined to create more comprehensive scenarios. This aspect is crucial during the selection of scenario sources.

A key challenge in scenario analysis is decision-making under deep uncertainty due to the lack of assigned probabilities to scenarios. While assigning probability can be difficult, it is possible for certain variables. For example, analyzing political trends over renewable energy perception can inform assumptions about subsidy policy evolution.

By assigning realistic probabilities to best and worst-case scenarios, mid-case scenarios can be used as representative of probabilities. With sufficient data, accurate scenario probability estimations are feasible.

This study integrates various scenarios to evaluate a single net present value (NPV) probability density function for the investment. This involves a three-step process:

1. Scenario Identification: construct or identify scenarios for regulatory, long-term market, and investment cost-related risks through literature review.
2. Scenario Selection: select the most probable scenarios.
3. NPV Function Aggregation: assess the NPV probability density function for each scenario, multiply these functions by their respective probabilities, and sum them.

This procedure is demonstrated in the case study example.

2.4. Risk Assessment

Net Present Value (NPV) is used as a measure of investment profitability over the project's lifespan. NPV is influenced by all the above cited uncertainties and their propagation effects. The NPV calculation involves nested uncertainty models, with each simulation run producing a specific NPV.

The investment cost (I_0) is initially calculated, then reduced based on learning effect scenarios, and finally sampled from a triangular distribution (centered on the model-calculated nominal value) using Monte Carlo simulation. Revenues are affected by energy price and power production uncertainties. Power production is subject to wind speed uncertainty (modeled using the Markov processes) and epistemic uncertainty of internal parameters (sampled from distributions). The randomly generated disruptions and failure list together with the related corrective maintenance costs impact operating costs. Monte Carlo sampling of bank and self-interest rates, along with the weighted average cost of capital (WACC), also introduce epistemic uncertainty, influencing both discounting and loan installments, as well as tax expenditures.

The simulation begins with the user selecting a location and turbine, populating the dataset with technical and environmental data. After defining constant inputs (number of runs, lifespan, etc.), the simulation starts.

Each run involves sampling epistemic uncertainty variables from their respective probability distributions. Stochastic processes are then simulated to generate annual time series for failures, wind speed, and electricity prices. This enables the calculation of annual net produced energy (excluding downtime). The economic model then calculates annual cash flows and the run-specific NPVs. Once all runs are terminated, the resulting NPV frequency distribution histogram is obtained.

Risk assessment involves:

- Computing the NPV probability density function.
- Evaluating the probability of NPV being less than zero.
- Assessing the Value at Risk (VaR), defined as the maximum economic loss with a 95% confidence level.
- Calculating the coefficient of variation in NPV as a measure of variability.

The NPV is computed using Equation (11), where I_0 is the investment cost; Y is the project lifespan; CF_y is the cash flow for year y; and WACC (Equation (12)) is the weighted average cost of capital.

$$NPV = -I_0 + \sum_{y=1}^{Y} \frac{CF_y}{(1 + WACC)^y} \tag{11}$$

$$WACC = c_0\left(\frac{I_0 - V_0}{I_0}\right) + c_d\left(\frac{V_0}{I_0}\right) \tag{12}$$

In the Weighted Average Cost of Capital (WACC) equation, V_0 represents the debt; c_d is the cost of debt; and c_0 is the cost of equity. The cash flow (CF_y) for year y is calculated using Equation (13), taking into account the yearly revenue, the yearly operating cost (OC_y), and taxes (T_y).

$$CF_y = R_y - OC_y - T_y \tag{13}$$

Taxes can be calculated using Equation (14), which considers the tax rate (a), the share interests of the debt (q_y), and the depreciation charge (AMM).

$$T_y = a\left[R_y - OC_y - q_y - AMM\right] \tag{14}$$

The loan installment (L), as shown in Equation (15), is assumed to be constant. Therefore, if V_{y-1} represents the outstanding debt from the previous year, the share interest can be calculated using Equation (16).

$$L = V_0 \frac{c_d(1 + c_d)^n}{(1 + c_d)^n - 1} \tag{15}$$

$$q_y = c_d V_{y-1} \tag{16}$$

In this context, n represents the total number of years for repaying the financed capital, as specified in the loan agreement.

2.5. Risk Hedging

Recognizing that uncertainty can negatively impact investment profitability, financial tools for risk hedging are integrated into the risk assessment model. Specifically, financial derivatives can be used for either speculation or risk mitigation. In renewable energy projects, investors typically prioritize risk hedging. Different energy markets necessitate varied hedging strategies, and practical guides exist for managing market uncertainty [74]. Electricity and weather-based swaps and forward contracts are commonly employed for mitigating risk, involving fixed prices per MWh for specified energy volumes [75,76], but even more complex instruments were proposed [77], such as vanilla options and derivatives. Given market volatility, research focuses on accurate pricing strategies for wind power futures [78] and power forward contracts [79]. To address prediction errors inherent in energy forecasting, weather derivatives based on forecast errors have been developed [80]. Real options theory has also been applied in wind farm feasibility studies [81]. To reduce computational complexity and maintain simplicity, an over-the-counter (OTC) contract was chosen for this study, despite the availability of other suitable financial instruments. The model's modular design allows for easy modification of this component (represented as the feedback arc in Figure 1) to incorporate a wider range of contracts. This model utilizes a forward contract, which involves selling a fixed volume (V) of energy to a single client at a predetermined strike price (St). The mathematical formulation of the forward price (F), considering that electricity is non-storable, is given in Equation (17).

$$F = V \cdot St \cdot e^{r \cdot t} \tag{17}$$

In Equation (17), r represents the risk-free rate of the investment, and t is the delivery date in years. Typically, the forward power price is a biased estimate of the future spot price. The forward premium decreases with the expected variance of wholesale spot prices and increases with their expected skewness.

In equilibrium, the forward price (F) is equal to the expected value of the spot price, minus the expected variance of spot prices multiplied by a positive parameter (k), plus the skewness of spot prices multiplied by another positive parameter (γ), as shown in Equation (18) [82]. These two parameters (k and γ) are typically chosen to reflect the risk aversion of investors.

$$F = E(St) - k \cdot var(St) + \gamma \cdot skew(St) \tag{18}$$

The negative correlation between expected spot price variance and forward premiums arises from risk-averse producers seeking to minimize price risk through forward contracts. On the other hand, a positive skewness indicates a higher probability of significant price increases, prompting risk-averse retailers to hedge against spot price volatility. Therefore, both producer and retailer hedging actions influence forward prices, pushing them down or up, respectively, as a safeguard against spot price uncertainty. While the preceding equations are used to estimate the forward price, buyer and seller estimations typically differ. Buyers anticipate price increases, while sellers anticipate decreases. This instrument allows sellers to hedge against energy price declines, and buyers to hedge against price increases. Buyers benefit when the fixed price exceeds the market price, and sellers benefit in the opposite scenario. The contract mandates the seller (energy producer) to supply a fixed energy quantity to the buyer, and the buyer to purchase it. Delivery occurs hourly, with each hour's volume determined by the ratio of total contract volume to the total hours between the contract's start and end dates. For contracts exceeding one year, the price is adjusted by capitalizing it using the risk-free cost of capital. If the producer cannot meet delivery requirements due to factors like low wind or turbine unavailability, they must supply all available energy and pay the buyer a penalty, as specified in the contract. This penalty is proportional to the undelivered power.

Overall, the computation for estimating the producer's cash flow related to the forward contract (FC) is as follows:

$$\begin{gathered} if\ EP_{yh} \geq V_{yh} : FC_y = FP \cdot V_{yh} \\ else : FC_y = FP \cdot EP_{yh} - FP_P(V_{yh} - EP_{yh}) \end{gathered} \tag{19}$$

In Equation (19), V_{yh} represents the hourly volume due; FP is the contracted electricity price per MWh; and FP_P is the contracted penalty.

After calculating the total energy produced by the wind farm in a given hour, if this quantity is less than or equal to the fixed volume specified in the contract, all energy is sold at the agreed strike price, and the corresponding penalty is calculated and paid to the buyer. Conversely, if the produced energy exceeds the contracted volume, only the contracted amount is sold at the strike price, while the excess energy is sold at the current market price. This forward contract instrument is incorporated into the revenue calculation process.

3. Application Example

The model's capabilities are showcased through its implementation in the MATLAB (Mathworks, rel. R2022a) environment and its application to a case study involving a 20-turbines wind farm. This proposed wind farm is situated roughly 5 km offshore from the port of Brindisi, Italy, at coordinates 40.68° latitude and 18.06° longitude (as depicted in Figure 4). The water depth at the site is approximately 400 m, and the anticipated investment date is 2030.

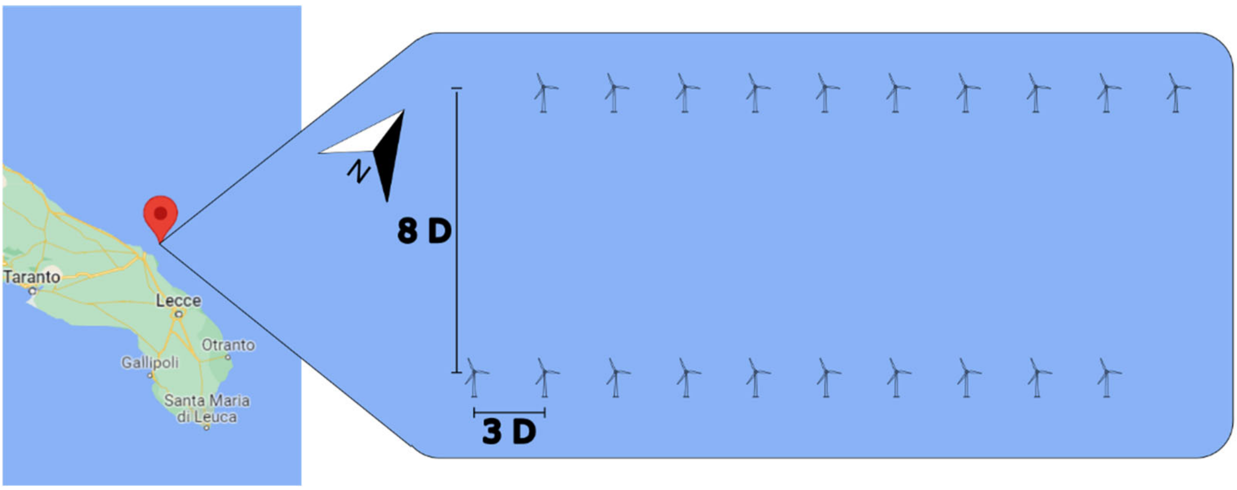

Figure 4. Hypothesized wind farm layout and site location.

For each turbine within the wind farm, a horizontal axis NREL 5-MW reference wind turbine [83] was selected, taking into account the specific site characteristics. This turbine is installed on a SPAR platform and has a rated wind speed of 11.4 m/s, with cut-in and cut-off speeds of 3 m/s and 25 m/s, respectively. Key specifications include a rotor diameter of 126 m and a hub height of 90 m. The turbine employs a geared drive train and operates using pitch regulation. The power curve and power coefficient for this turbine are detailed in Figure 5.

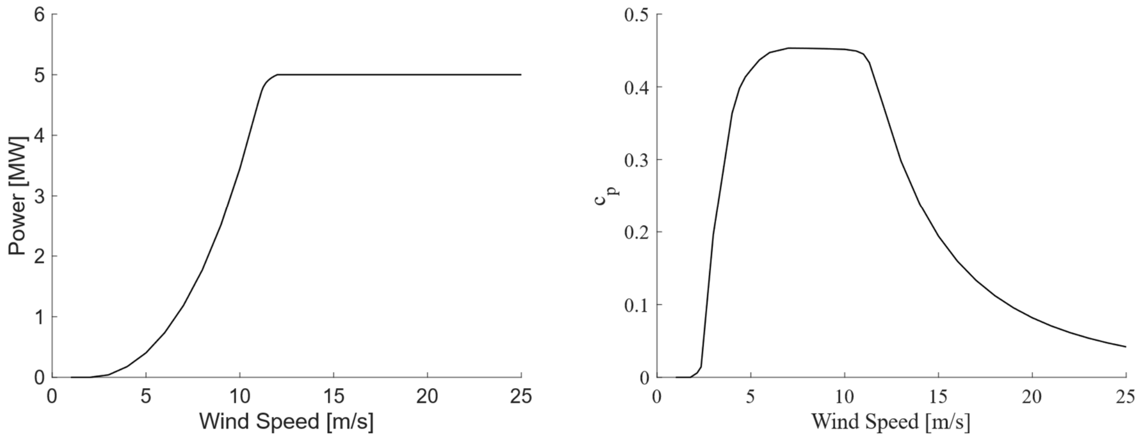

Figure 5. Five MW wind turbine power curve and power coefficient.

Turbines are arranged in two rows with a horizontal spacing of three rotor diameters and a vertical spacing of eight rotor diameters. This specific layout was adopted based on indications from references [52,53] to reduce the adverse effects of turbine wakes on energy production. Figure 6 illustrates the percentage of waked area for a representative turbine (the fifth in the front row, facing north) as a function of wind direction. As the figure demonstrates, southerly winds result in shadowing from the second row, while winds from the east or west lead to wake effects from turbines within the same row.

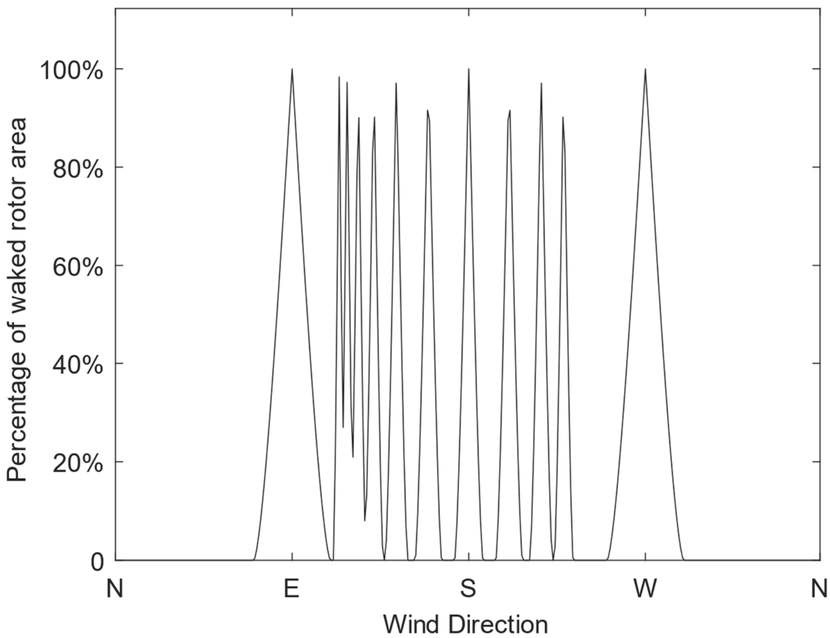

Figure 6. Percentage of waked rotor area in the function of wind direction.

The site-specific wind direction distribution is represented by the wind rose shown in Figure 7.

Hourly wind speed and direction data at a height of 10 m were obtained from the ECMWF ERA5-Land dataset, covering the period from 2015 to 2019. These historical data were utilized to define the states and transition probabilities of a Markov chain model. This model was subsequently employed to generate synthetic hourly wind speed values for the projected operational lifespan of the wind farm, which were then adjusted to the turbine hub height using a logarithmic wind profile. The average wind speed over the twenty-year operational period is calculated to be 5.89 m/s, and the coefficient of variation in the historical wind speed time series is 0.55. Furthermore, the maximum wind speed in the generated synthetic data are 18 m/s, consistent with the historical record. The specific methodology for wind speed time series generation and energy price modeling follows the approach detailed in reference [35]. A comparison between a sample of the generated synthetic wind speed time series and actual historical data are presented in Figure 8.

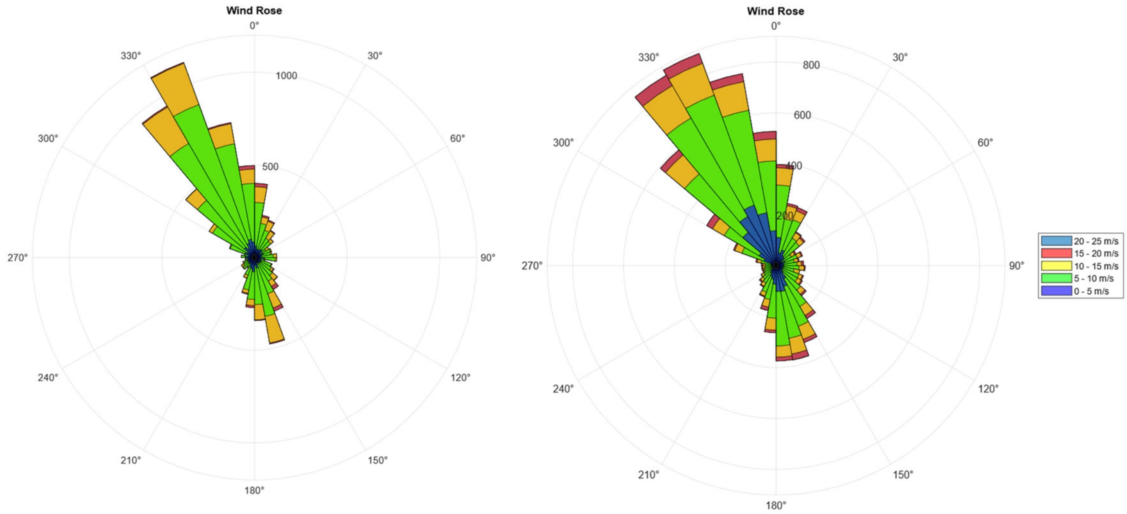

Figure 7. Real data wind rose (**left side**) and simulated data wind rose for the first year of a generic run (**right side**).

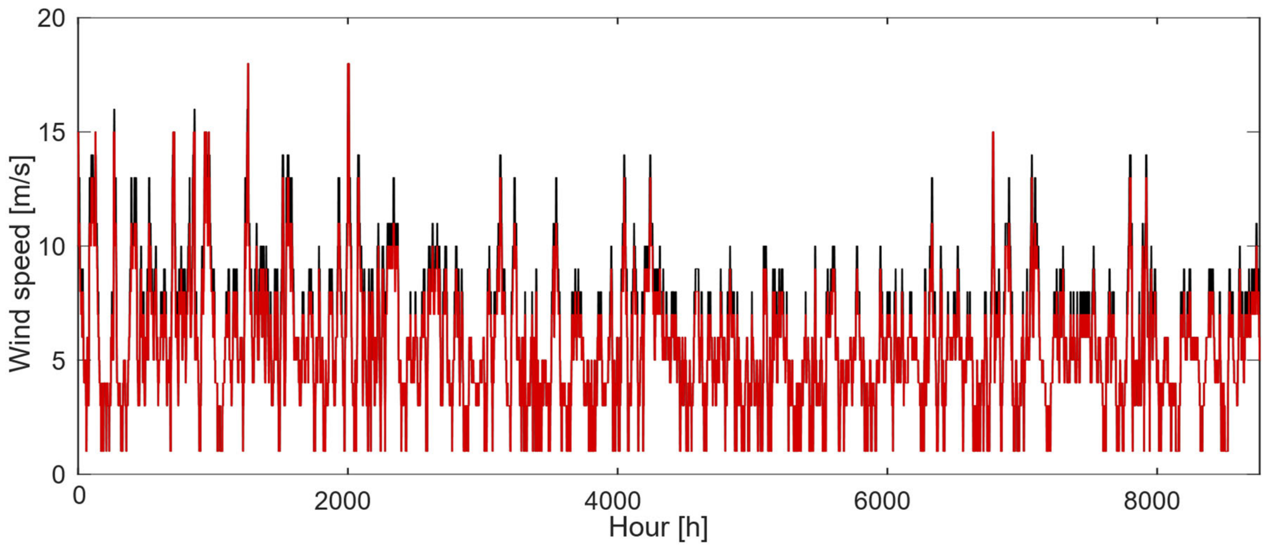

Figure 8. Sample comparison between real wind speed data (red line) and a simulated wind speed time series generated for a generic simulated year.

The instantaneous power output of each turbine was determined based on the simulated wind speed, utilizing Equation (1) and the power curve and power coefficient characteristics of the selected reference turbine type, as illustrated in Figure 5. The estimation of structural costs for the SPAR floating platform was based on geometrical and construction details sourced from Castro-Santos [56], in conjunction with the adopted cost model. This same cost model was applied to estimate the wind turbine costs, utilizing the previously specified turbine data. Distance-dependent costs were evaluated considering the defined wind farm layout and its geographical location. The primary outcomes of the cost estimation process are summarized in Table 3. The expected investment cost, initially calculated based on 2013 values and presented in Table 3, was adjusted to reflect present value considerations by applying the current European Union Producer Price Index (PPI). Given a European PPI of 103.7 in 2013 and 133.6 at the beginning of 2023 [84], this correction results in an approximate 30% increase in the cost figures.

Table 3. Main items costs calculated by the model.

Cost Item	**Nominal Value**
Wind turbines	EUR 157.4 M
Floating platforms	EUR 92.0 M
Transmission systems	EUR 29.3 M
Mooring and anchoring systems	EUR 36.5 M
Wind turbines installation	EUR 13.0 M
Floating platforms installation	EUR 13.9 M
Mooring and anchoring systems installation	EUR 1.4 M
Transmission systems installation	EUR 3.5 M
Total Investment Cost	EUR 347 M

The three scenarios are designated as High Investment Cost Reduction (H), Medium Investment Cost Reduction (M), and Low Investment Cost Reduction (L). The extent of investment cost reduction within each scenario is predicated on the projected European installed offshore wind capacity by the year 2030. A constant learning rate of 9% is assumed across all scenarios. However, the total European installed capacity in 2030 is varied, with values of 40.5 GW, 70.2 GW, and 98.93 GW, corresponding to the L, M, and H scenarios, respectively. These values are informed by forecasted developments in the energy economy over the coming years. The L scenario posits limited advancements in electricity interconnections among European nations, the persistence of unfavorable national policies concerning permitting and planning in high-potential markets, and the non-achievement of the European renewable energy target. The M scenario envisions the establishment of regional cooperation mechanisms, the full implementation of the renewable energy directive, and the strengthening of national policies supportive of wind energy, alongside an intensification of power interconnection infrastructures. The H scenario assumes an increase in the European targets for renewable energy sources (RES) to 35%, a greater intensification of the power transmission network beyond the initial 15% target, and an acceleration in new installations driven by favorable policies enacted by member states. Consequently, based on these underlying assumptions and the assumed learning curve (see Figure 3), the projected investment cost reductions for scenarios H, M, and L are approximately 23%, 17%, and 12%, respectively.

Regarding the estimation of electricity sale revenues, a time series of energy prices is required. To this end, the hourly time series of the Italian energy price for the year 2021, obtained from the GME (Gestore dei Mercati Energetici) database, was utilized to estimate the parameters of an Autoregressive Integrated Moving Average (ARIMA) regression model. This model was subsequently employed to simulate wind speed values throughout the operational lifespan of the wind plant. In addition to capturing short-term price variability, as illustrated in Figure 9, the model also incorporates a long-term trend component that influences the average base price, with three distinct paths depicted in Figure 10.

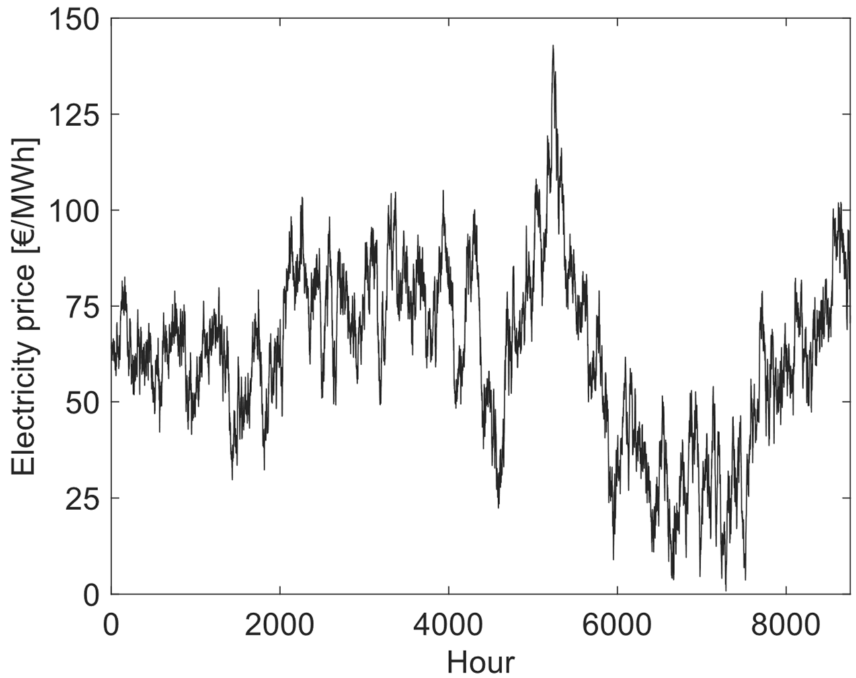

Figure 9. Example of simulated time series of electricity price for one year of plant's life.

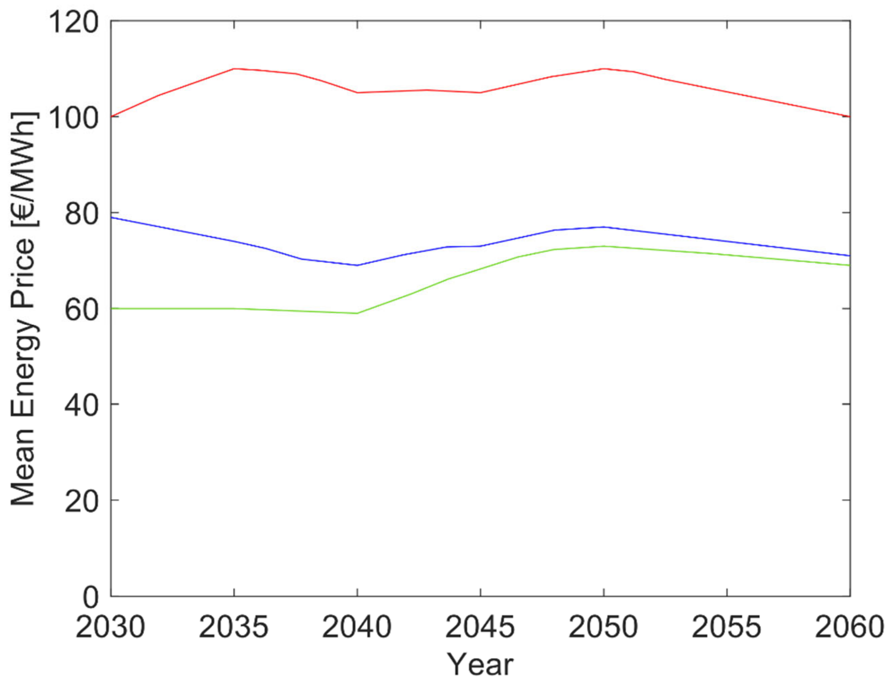

Figure 10. Mean energy price during years according to the T scenario (red line), C scenario (blue line), and R scenario (green line).

Energy price scenarios, based on the methodology of Schmitt and Zhou [73], were developed to encompass a range of potential future market conditions. Three distinct scenarios were selected: Relief (R), Central (C), and Tension (T). Beyond traditional energy market factors, the analysis incorporates considerations of the prevailing geopolitical landscape. The Relief scenario posits a de-escalation of tensions among the USA, Europe, Russia, and China, anticipating continued fossil fuel imports from Russian pipelines and a consequent reduction in energy prices. However, an ongoing effort to lessen dependence on Russia is assumed, leading to a decrease in natural gas imports compared to pre-2021 levels, while recently adopted renewable energy targets remain in effect. The Central scenario envisions Europe ceasing the import of Russian pipeline gas by 2027, coupled with a gradual increase in the utilization of renewable energy sources in subsequent years. Natural gas is progressively replaced by synthetic fuels, such as green hydrogen, and the price of natural gas declines to maintain competitiveness. Furthermore, an increased adoption of heat pumps is projected, with electric vehicles and trucks accounting for 95% of the European market by 2060. The Tension scenario assumes the continuation and potential escalation of current tensions between Russia and the West, resulting in an increase in energy prices. Europe immediately halts the importation of Russian pipeline gas, and European consumers face competition with Asian markets for available energy resources.

Regulatory risk is addressed through the consideration of subsidy scenarios. Despite the current absence of subsidies for offshore wind power plants at the time of this study, the potential introduction of a subsidy plan by the Italian government is considered. Three scenarios were analyzed: feed-in tariff (F), feed-in premium tariff (P), and no subsidies (N). In the feed-in tariff scenario, the lack of specific data led to the adoption of a tariff of EUR 187/MWh, based on the historical levelized cost of energy for offshore wind power systems [85]. Under this scenario, the time series of electricity prices does not influence the NPV, as the generated power is sold at a fixed price. In the feed-in premium tariff scenario, a fixed premium of EUR 31/MWh is applied, which is added to the prevailing market price of energy to determine the selling price. In the no-subsidies scenario, the selling price is solely determined by the current energy market price, without any supplementary subsidies or premiums.

The defined scenarios are grouped into three groups, corresponding to each scenario driver: mean electricity price, subsidies, and learning effect. Within each group, the scenarios are mutually exclusive. It is worthwhile to point out that the selection of the feed-in tariff subsidy renders the NPV probability density function independent of energy price fluctuations, although it remains sensitive to investment cost reductions. This framework results in a total of twenty-one possible scenario permutations. The energy price scenarios and investment cost scenarios are informed by European energy scenarios projected to 2050. The primary driver of the energy price scenarios is the geopolitical relationship between Western and Eastern countries, while the investment cost scenarios are largely influenced by the internal policies of European member states. Conversely, the subsidy scenarios are primarily determined by the internal policy decisions of Italy. These assumptions of primary drivers warrant for independence among the evolutions of the referred variables, thereby enabling the consideration of all permissible permutations. Nevertheless, to make the analysis more manageable for illustrative purposes, a scenario reduction process was implemented resorting to the concept of the plausibility cone [86–89], which allowed to establish a narrowed range of scenarios deemed plausible within the defined context.

The assumed scenarios were subdivided into four categories: preferable, possible, plausible, and probable. While scenarios HF, MF, and LF may be considered preferable from the perspective of a wind power investor, they are not classified as probable. This is due to the global trend in subsidy policies shifting towards feed-in premium tariffs rather than feed-in tariffs. However, among the set of three scenarios, LF remains the most plausible option, predicated on the rationale that lower investment cost reductions may prompt regulators to adopt more effective subsidy policies. Furthermore, current geopolitical developments suggest a continuation of non-relief conditions between Western and Eastern countries, indicating that scenarios assuming relief (R) are possible rather than probable. Given that the worst-case tension scenario (T) serves as a boundary for the analysis, the central scenario (C) emerges as the most probable energy price scenario. While scenarios with no subsidies (N) are plausible, the apparent inclination of Italian policymakers towards implementing subsidies, particularly for wind and solar energy, places scenarios involving feed-in premium subsidies within the probable group. Moreover, considering ongoing global and European investments in wind power systems, a significant reduction in investment costs is deemed highly probable, leading to the classification of the High Investment Cost Reduction (HCP) scenario as the most probable future outcome, if current sourcing difficulties [2] are considered contingent. Based on statements and projections from European and Italian governmental bodies regarding renewable energy sources capacity installation trends, and anticipated advancements in wind power technology, four distinct narratives on subsidy policy development were considered (representing the treatment of Type IV uncertainty in this application example). Simulation results were subsequently combined, weighted by their respective probabilities, to derive a consolidated probability density function for the NPV. The NPV density function for each scenario was evaluated individually and then multiplied by its associated probability. Finally, these individual results were summed up to obtain the overall NPV probability density function. The plant's life cycle was divided into six timespans, to account for its dynamic evolution, each characterized by a specific percentage change in the feed-in premium tariff value, as detailed in Table 4.

Table 4. Time span percentage change in feed-in premium tariff value.

Probability	**Time Span**					
	1	**2**	**3**	**4**	**5**	**6**
35%	0%	0%	0%	0%	0%	0%
5%	5%	10%	15%	20%	25%	25%
20%	−5%	−30%	−50%	−60%	−70%	−70%
40%	0%	0%	−70%	−70%	−70%	−70%

A Monte Carlo simulation was employed to address epistemic uncertainty in each variable, utilizing symmetrical triangular distributions. The range of these distributions (minimum and maximum values) was defined for most variables based on a percentual deviation (PD) from the nominal value: nominal ± (PD × nominal). Exceptions were the bank interest rate, modeled with an absolute deviation of ±4% around a nominal 6%, and the self-interest rate, with an absolute deviation of ±2% around a nominal 4%. Table 5 provides the nominal values and the adopted PD, informed by [90,91]. The analysis also assumes a 10-year financial loan covering 50% of the investment, a 35% tax rate, a technician hourly cost of EUR 50, and an annual amortization rate of 7%.

Table 5. Parameters for variables showing epistemic uncertainty.

Variable	**Nominal Value**	**PD**
Power coefficient	See curve in Figure 5	±1%
Generator efficiency	See curve in Figure 11	±1%
Power electronic efficiency	See curve in Figure 11	±1%
Gearbox efficiency	98%	±1%
Restoration Cost	See [7]	±10%
Investment cost	EUR 350 M	±30%
Plant years life	20 (nominal)	±10%

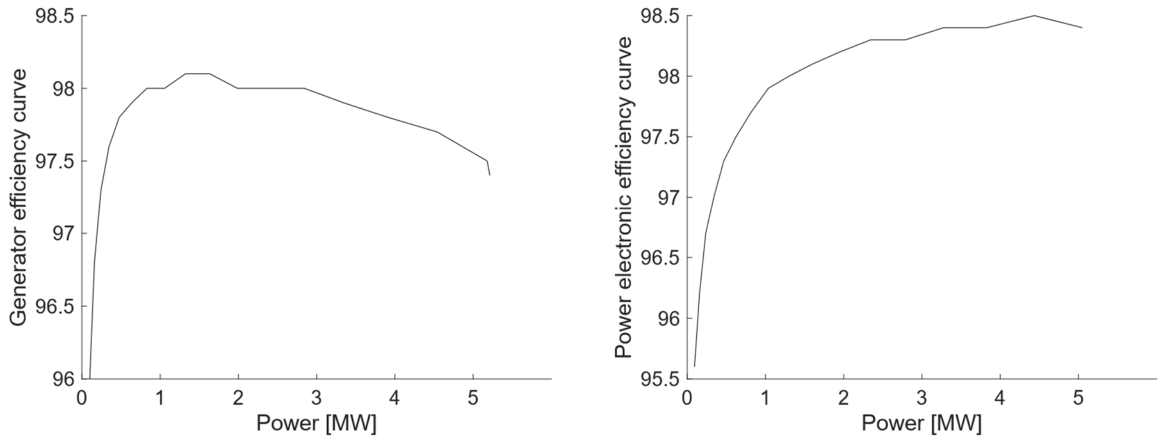

Figure 11. Generator and power electronic efficiency curves.

Failure events were modeled using data on average failure rates, repair times, repair costs, and technician requirements (by component and damage level) derived from [7], and failure histories were generated using the method outlined in [35]. Repair costs from [7] were increased by 10% to account for the larger turbine size compared to the 2–4 MW turbines the data originally referenced, and these costs were also adjusted for inflation using the European Producer Price Index. The risk of earthquake-related disruptions was considered negligible for the chosen site and adopted floating platform and was therefore not included in the failure modeling. To address risk hedging in the analyzed scenario, the key assumptions regarding the forward contract are summarized in Table 6.

Table 6. Forward contract assumptions.

Expiring Date	2042
Starting date	2030
Strike price	EUR 130/MWh
Yearly volume	50 GWh
Risk-free rate	1.5%
Penalty per MWh	EUR 20/MWh

Figure 12 illustrates the frequency distribution of the Net Present Value obtained from 1000 iterations of the system analysis. The distribution exhibits an average NPV of around EUR 8 million and a standard deviation of EUR 11 million, with observed values ranging from a maximum of EUR 43 million to a minimum of EUR −18 million. The 5% Value at Risk (VaR) is EUR −9 million, implying a low probability (less than 5%) of losses exceeding this amount. Nevertheless, the probability of the NPV being negative, signifying an economic loss, is 24%. Further details on the NPV and associated risk metrics are available in Table 7.

A comparison of the net present value (NPV) distribution and cumulative probability between a single wind turbine system and a 20-turbine wind farm is illustrated in Figure 13. To facilitate this comparison, the original dataset was maintained, with the exception of the future contract's yearly volume, which was reduced twenty-fold for the single turbine scenario. The distributions presented were generated using MATLAB's distribution fitter with a 95% confidence level. The results indicate that investing in a single wind turbine in the Mediterranean region is not cost-effective due to the low average wind speeds, yielding an expected NPV of EUR −2.2 million against an investment of around EUR 25.5 million. In contrast, the 20-turbine wind farm benefits from economies of scale and increased system availability due to the redundancy of multiple independent turbines, which more than offset the losses from wake effects, ultimately resulting in a cost-effective investment despite the low average wind speeds.

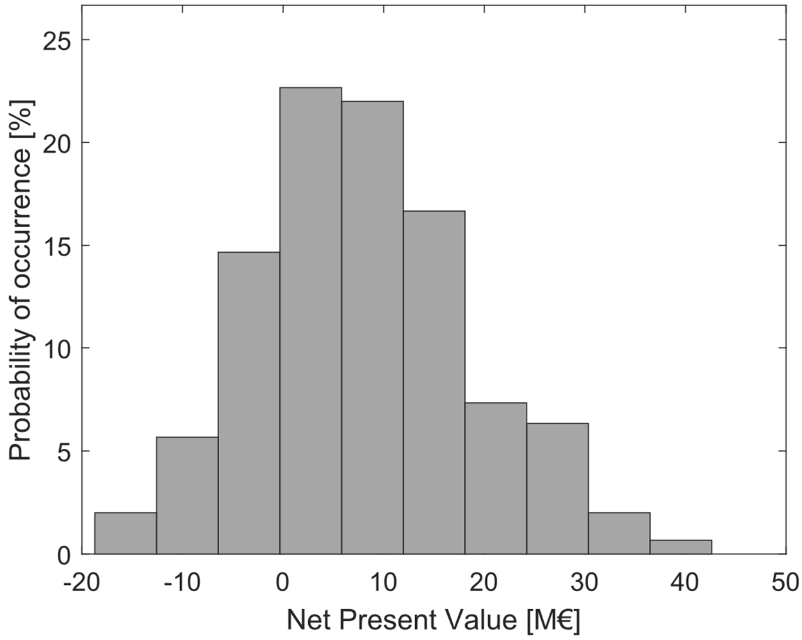

Figure 12. Net present value frequency distribution of considered wind farm.

Table 7. Profitability and risk analysis results.

Min Data Value	EUR $-1.87 \cdot 10^7$
Max Data Value	EUR $4.26 \cdot 10^7$
E [NPV]	EUR $7.99 \cdot 10^6$
σ	EUR $1.09 \cdot 10^7$
CV	1.37
P (NPV < 0)	24.00%
VaR 5%	EUR $-9.04 \cdot 10^6$

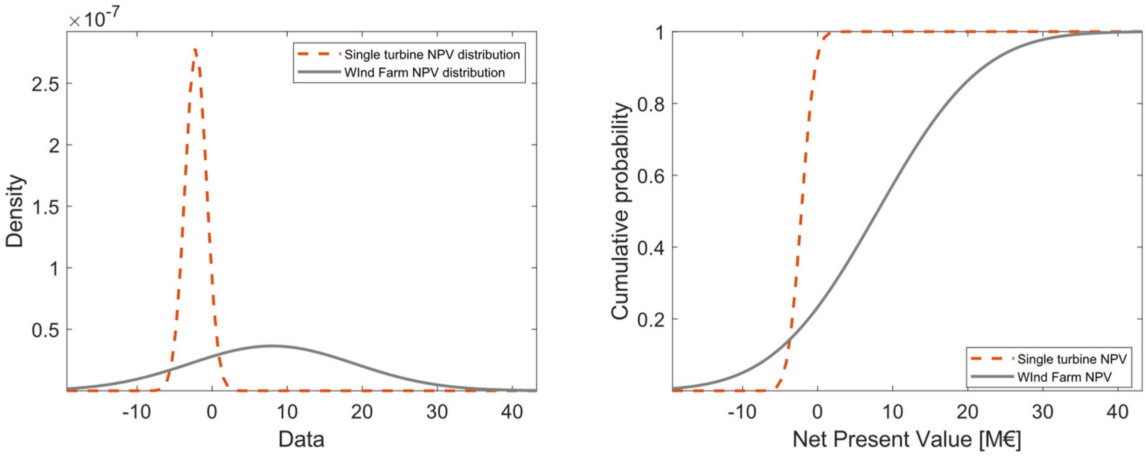

Figure 13. Net present value probability distribution (**left side**) and cumulative probability of net present value (**right side**).

4. Conclusions

This paper introduces a comprehensive framework for evaluating the economics and risks of offshore wind farms, addressing a notable gap in the literature. Unlike prior work that often neglects uncertainty or examines a limited number of variables in isolation (e.g., static Monte Carlo, one-at-a-time sensitivity), our model offers an integrated assessment of diverse uncertainty sources across short and long-term horizons, specifically for wind farms. It uniquely incorporates economies of scale in capital investment, accounts for wake effect interference on energy production, models scenario changes throughout the project lifecycle, and includes financial derivatives for risk hedging.

A numerical application demonstrates the critical importance of considering uncertainty propagation, revealing a significant probability of financial losses despite a positive average NPV under nominal conditions for the examined example. While currently limited to a single financial instrument and focusing on electricity market risk (with disruptive events limited to earthquakes), future work will expand the model to include a broader range of financial hedging tools (swaps, futures, weather risk), broader market conditions (e.g., liquidity constraints), and additional disruptive events (rogue waves, hurricanes, ship collisions), as well as long-term climate change impacts on wind resources and extreme weather. Furthermore, the environmental impact on precipitation and maritime traffic risks associated with offshore platforms warrant further investigation. Additionally, investment growth and construction delay risk resulting from an increase in commodities prices and sourcing problems due to supply chains instabilities will be modeled. Ultimately, this model serves as a valuable decision support tool for the planning phase of offshore wind investments, enabling risk-aware profitability evaluations and facilitating the comparison of alternative design choices. Its modularity also allows for application during the operation phase to test maintenance policies and production control strategies based on real-time forecast of wind and energy prices. This study contributes a more detailed and comprehensive approach to offshore wind farm investment assessment and supports risk-informed decision-making throughout the project's entire lifecycle.

Author Contributions: Conceptualization, A.C.C.; methodology, A.C.C., A.F., P.M.P. and P.S.; software, A.F.; validation, A.F.; formal analysis, A.C.C., A.F., P.M.P. and P.S.; investigation, A.C.C., A.F. and P.S.; resources, P.S.; data curation, A.F.; writing—original draft preparation, A.C.C. and A.F.; writing—review and editing, A.C.C.; visualization, A.F. and P.S.; supervision, A.C.C. All authors have read and agreed to the published version of the manuscript.

Funding: This research received no external funding.

Data Availability Statement: Data will be made available on request.

Conflicts of Interest: The authors declare no conflict of interest.

References

1. Nghiem, A.; Pineda, I. *Wind Energy in Europe: Scenarios for 2030*; WindEurope: Brussels, Belgium, 2017; Volume 30, p. 32. Available online: https://windeurope.org/wp-content/uploads/files/about-wind/reports/Wind-energy-in-Europe-Scenarios-for-2030.pdf (accessed on 13 February 2025).
2. McKinsey, Co. Offshore Wind: Strategies for Uncertain Times. 12 July 2024. Available online: https://www.mckinsey.com/industries/electric-power-and-natural-gas/our-insights/offshore-wind-strategies-for-uncertain-times (accessed on 13 February 2025).
3. Apak, S.; Atay, E.; Tuncer, G. Financial risk management in renewable energy sector: Comparative analysis between the European Union, Turkey. *Procedia-Soc. Behav. Sci.* **2011**, *24*, 935–945. [CrossRef]
4. Lee, C.W.; Zhong, J. Financing and risk management of renewable energy projects with a hybrid bond. *Renew. Energy* **2015**, *75*, 779–787. [CrossRef]

5. Shafiee, M.; Sørensen, J.D. Maintenance optimization and inspection planning of wind energy assets: Models, methods and strategies. *Reliab. Eng. Syst. Saf.* **2019**, *192*, 105993. [CrossRef]
6. Faulstich, S.; Hahn, B.; Tavner, P.J. Wind turbine downtime and its importance for offshore deployment. *Wind Energy* **2011**, *14*, 327–337. [CrossRef]
7. Carroll, J.; McDonald, A.; McMillan, D. Failure rate, repair time and unscheduled O&M cost analysis of offshore wind turbines. *Wind Energy* **2016**, *19*, 1107–1119.
8. Castro-Santos, L.; Silva, D.; Bento, A.R.; Salvação, N.; Soares, C.G. Economic feasibility of floating offshore wind farms in Portugal. *Ocean Eng.* **2020**, *207*, 107393. [CrossRef]
9. Castro-Santos, L.; Filgueira-Vizoso, A.; Carral-Couce, L.; Formoso, J.A.F. Economic feasibility of floating offshore wind farms. *Energy* **2016**, *112*, 868–882. [CrossRef]
10. Gaß, V.; Strauss, F.; Schmidt, J.; Schmid, E. Economic assessment of wind power uncertainty. In Proceedings of the World Renewable Energy Congress-Sweden, Linköping, Sweden, 8–13 May 2011; Linköping University Electronic Press: Linköpin, Sweden, 2011; pp. 4169–4176. Available online: https://ep.liu.se/ecp/057/vol15/016/ecp57vol15_016.pdf (accessed on 13 February 2025).
11. Vardar, A.; Çetïn, B. Cost Assessment of the Possibility of Using Three Types of Wind Turbine in Turkey. *Energy Explor. Exploit.* **2007**, *25*, 71–82. [CrossRef]
12. Khindanova, I. A Monte Carlo model of a wind power generation investment. *J. Appl. Bus. Econ.* **2013**, *15*, 94–106.
13. Ma, X.-Y.; Sun, Y.-Z.; Fang, H.-L. Scenario Generation of Wind Power Based on Statistical Uncertainty and Variability. *IEEE Trans. Sustain. Energy* **2013**, *4*, 894–904. [CrossRef]
14. Sohoni, V.; Gupta, S.C.; Nema, R.K. A Critical Review on Wind Turbine Power Curve Modelling Techniques and Their Applications in Wind Based Energy Systems. *J. Energy* **2016**, *2016*, 8519785. [CrossRef]
15. Petrone, G.; de Nicola, C.; Quagliarella, D.; Witteveen, J.; Iaccarino, G. Wind turbine performance analysis under uncertainty. In Proceedings of the 49th AIAA Aerospace Sciences Meeting including the New Horizons Forum and Aerospace Exposition, Orlando, FL, USA, 4–7 January 2011; p. 544.
16. Ali, M.; Matevosyan, J.; Milanović, J. Probabilistic assessment of wind farm annual energy production. *Electr. Power Syst. Res.* **2012**, *89*, 70–79. [CrossRef]
17. Sakki, G.; Tsoukalas, I.; Kossieris, P.; Makropoulos, C.; Efstratiadis, A. Stochastic simulation-optimization framework for the design and assessment of renewable energy systems under uncertainty. *Renew. Sustain. Energy Rev.* **2022**, *168*, 112886. [CrossRef]
18. Egli, F. Renewable energy investment risk: An investigation of changes over time and the underlying drivers. *Energy Policy* **2020**, *140*, 111428. [CrossRef]
19. Xu, Y.; Du, R.; Pei, J. The investment risk evaluation for onshore and offshore wind power based on system dynamics method. *Sustain. Energy Technol. Assess.* **2023**, *58*, 103328. [CrossRef]
20. Erfani, A.; Tavakolan, M. Risk Evaluation Model of Wind Energy Investment Projects Using Modified Fuzzy Group Decision-making and Monte Carlo Simulation. *Arthaniti J. Econ. Theory Pract.* **2020**, *22*, 7–33. [CrossRef]
21. Gatzert, N.; Kosub, T. Risks and risk management of renewable energy projects: The case of onshore and offshore wind parks. *Renew. Sustain. Energy Rev.* **2016**, *60*, 982–998. [CrossRef]
22. Onar, S.Ç.; Kılavuz, T.N. Risk Analysis of Wind Energy Investments in Turkey. *Hum. Ecol. Risk Assess. Int. J.* **2015**, *21*, 1230–1245. [CrossRef]
23. Lei, X.; Shiyun, T.; Yanfei, D.; Yuan, Y. Sustainable operation-oriented investment risk evaluation and optimization for renewable energy project: A case study of wind power in China. *Ann. Oper. Res.* **2020**, *290*, 223–241. [CrossRef]
24. Herbert-Acero, J.F.; Probst, O.; Réthoré, P.-E.; Larsen, G.C.; Castillo-Villar, K.K. A Review of Methodological Approaches for the Design and Optimization of Wind Farms. *Energies* **2014**, *7*, 6930–7016. [CrossRef]
25. Pires, A.L.G.; Junior, P.R.; Morioka, S.N.; Rocha, L.C.S.; Bolis, I. Main Trends and Criteria Adopted in Economic Feasibility Studies of Offshore Wind Energy: A Systematic Literature Review. *Energies* **2021**, *15*, 12. [CrossRef]
26. Yilmazlar, K.; White, C.; Cacciola, S.; Candido, J.; Croce, A. Cost modelling for offshore wind farms using dynamic cost functions and engineering wake models. In Proceedings of the EERA DeepWind Conference 2023, Trondheim, Norway, 18–20 January 2023.
27. Borràs Mora, E.; Spelling, J.; van der Weijde, H. Transition from deterministic to stochastic cost models for offshore wind farms. In Proceedings of the Offshore Wind Energy Conference, London, UK, 6–8 June 2017.
28. Mora, E.B.; Spelling, J.; van der Weijde, A.H.; Pavageau, E.-M. The effects of mean wind speed uncertainty on project finance debt sizing for offshore wind farms. *Appl. Energy* **2019**, *252*, 113419. [CrossRef]
29. Mora, E.B.; Spelling, J.; van der Weijde, A.H. Global sensitivity analysis for offshore wind cost modelling. *Wind Energy* **2021**, *24*, 974–990. [CrossRef]
30. Ioannou, A.; Angus, A.; Brennan, F. Stochastic Prediction of Offshore Wind Farm LCOE through an Integrated Cost Model. *Energy Procedia* **2017**, *107*, 383–389. [CrossRef]

31. Rinaldi, G.; Garcia-Teruel, A.; Jeffrey, H.; Thies, P.R.; Johanning, L. Incorporating stochastic operation and maintenance models into the techno-economic analysis of floating offshore wind farms. *Appl. Energy* **2021**, *301*, 117420. [CrossRef]
32. Dinwoodie, I.; McMillan, D.; Revie, M.; Lazakis, I.; Dalgic, Y. Development of a Combined Operational and Strategic Decision Support Model for Offshore Wind. *Energy Procedia* **2013**, *35*, 157–166. [CrossRef]
33. Lee, J.C.Y.; Fields, M.J. An overview of wind-energy-production prediction bias, losses, and uncertainties. *Wind Energy Sci.* **2021**, *6*, 311–365. [CrossRef]
34. Yan, J.; Möhrlen, C.; Göçmen, T.; Kelly, M.; Wessel, A.; Giebel, G. Uncovering wind power forecasting uncertainty sources and their propagation through the whole modelling chain. *Renew. Sustain. Energy Rev.* **2022**, *165*, 112519. [CrossRef]
35. Caputo, A.C.; Federici, A.; Pelagagge, P.M.; Salini, P. Offshore wind power system economic evaluation framework under aleatory and epistemic uncertainty. *Appl. Energy* **2023**, *350*, 121585. [CrossRef]
36. Connolly, D.; Lund, H.; Mathiesen, B.; Leahy, M. A review of computer tools for analysing the integration of renewable energy into various energy systems. *Appl. Energy* **2010**, *87*, 1059–1082. [CrossRef]
37. EMD International A/S. energyPro. Available online: https://www.emd-international.com/energypro/ (accessed on 13 February 2025).
38. HOMER. UL Solution. Available online: https://www.homerenergy.com/ (accessed on 13 February 2025).
39. Natural Resources Canada, Government of Canada. RETScreen. Available online: https://www.retscreen.net/ (accessed on 13 February 2025).
40. National Renewable Energy Laboratory. System Advisor Model SAM. Available online: https://sam.nrel.gov/ (accessed on 13 February 2025).
41. Mathew, S. *Wind Energy: Fundamentals, Resource Analysis and Economics*; Springer: Berlin/Heidelberg, Germany, 2006.
42. Veena, R.; Manuel, S.; Mathew, S.; Petra, M. Wake Induced Power Losses in Wind Farms. *Int. J. Eng. Adv. Technol.* **2020**, *9*, 2175–2180.
43. Barthelmie, R.J.; Hansen, K.; Frandsen, S.T.; Rathmann, O.; Schepers, J.; Schlez, W.; Phillips, J.; Rados, K.; Zervos, A.; Politis, E.S.; et al. Modelling and measuring flow and wind turbine wakes in large wind farms offshore. *Wind Energy Int. J. Prog. Appl. Wind Power Convers. Technol.* **2009**, *12*, 431–444. [CrossRef]
44. Gaumond, M.; Réthoré, P.-E.; Bechmann, A.; Ott, S.; Larsen, G.C.; Diaz, A.P.; Hansen, K.S. Benchmarking of wind turbine wake models in large offshore wind farms. In Proceedings of the Science of Making Torque from Wind Conference, Oldenburg, Germany, 9–11 October 2012.
45. González-Longatt, F.; Wall, P.; Terzija, V. Wake effect in wind farm performance: Steady-state and dynamic behavior. *Renew. Energy* **2012**, *39*, 329–338. [CrossRef]
46. Rahbari, O.; Raahemifar, K.; Rosen, M.; Varzandeh, M.H.M.; Vafaeipour, M. Developing Realistic Designs for Wind Farms: Incorporation of an Imperialist Competitive Algorithm. In Proceedings of the 4th World Sustainability Forum, Basel, Switzerland, 1–30 November 2014.
47. Kaldellis, J.K.; Triantafyllou, P.; Stinis, P. Critical evaluation of Wind Turbines' analytical wake models. *Renew. Sustain. Energy Rev.* **2021**, *144*, 110991. [CrossRef]
48. Wei, D.; Zhao, W.; Wan, D.; Xiao, Q. A new method for simulating multiple wind turbine wakes under yawed conditions. *Ocean Eng.* **2021**, *239*, 109832. [CrossRef]
49. Jensen, N.O. *A Note on Wind Generator Interaction*; Risø National Laboratory: Roskilde, Denmark, 1983; Risø-M No. 2411.
50. Katic, I.; Højstrup, J.; Jensen, N.O. A simple model for cluster efficiency. In *European Wind Energy Association Conference and Exhibition*; A. Raguzzi: Rome, Italy, 1986; pp. 407–410.
51. Shakoor, R.; Hassan, M.Y.; Raheem, A.; Wu, Y.-K. Wake effect modeling: A review of wind farm layout optimization using Jensen's model. *Renew. Sustain. Energy Rev.* **2016**, *58*, 1048–1059. [CrossRef]
52. Ackermann, T. *Wind Power in Power Systems*; John Wiley & Sons: Hoboken, NJ, USA, 2012.
53. Schwanz, D.; Henke, R.E.; Leborgne, R.C. Wind power integration in Southern Brazil: Steady-state analysis. In Proceedings of the 2012 6th IEEE/PES Transmission and Distribution: Latin America Conference and Exposition (T&D-LA), Montevideo, Uruguay, 3–5 September 2012; pp. 1–6.
54. Altman, N.S. An Introduction to Kernel and Nearest-Neighbor Nonparametric Regression. *Am. Stat.* **1992**, *46*, 175–185. [CrossRef]
55. Maienza, C.; Avossa, A.; Ricciardelli, F.; Coiro, D.; Troise, G.; Georgakis, C. A life cycle cost model for floating offshore wind farms. *Appl. Energy* **2020**, *266*, 114716. [CrossRef]
56. Castro-Santos, L. *Methodology Related to the Development of the Economic Evaluation of Floating Offshore Wind Farms in Terms of the Analysis of the Cost of their Life-Cycle Phases*; Universidade da Coruña: A Coruña, Spain, 2013; ISBN 846165188X; 9788461651887.
57. Castro-Santos, L.; Filgueira-Vizoso, A.; Lamas-Galdo, I.; Carral-Couce, L. Methodology to calculate the installation costs of offshore wind farms located in deep waters. *J. Clean. Prod.* **2018**, *170*, 1124–1135. [CrossRef]
58. Lgen, K.; Hepbasli, A. Determination of Weibull parameters for wind energy analysis of ?zmir, Turkey. *Int. J. Energy Res.* **2002**, *26*, 495–506.

59. Ajayi, O.O.; Fagbenle, R.O.; Katende, J.; Ndambuki, J.M.; Omole, D.O.; Badejo, A.A. Wind Energy Study and Energy Cost of Wind Electricity Generation in Nigeria: Past and Recent Results and a Case Study for South West Nigeria. *Energies* **2014**, *7*, 8508–8534. [CrossRef]
60. Kwon, S.-D. Uncertainty analysis of wind energy potential assessment. *Appl. Energy* **2010**, *87*, 856–865. [CrossRef]
61. Negra, N.B.; Holmstrøm, O.; Bak-Jensen, B.; Sørensen, P. Model of a synthetic wind speed time series generator. *Wind. Energy Int. J. Prog. Appl. Wind Power Convers. Technol.* **2008**, *11*, 193–209. [CrossRef]
62. Patel, M.R.; Beik, O. *Wind and Solar Power Systems: Design, Analysis, and Operation*; CRC Press: Boca Raton, FL, USA, 2021.
63. Huang, Y.-N.; Whittaker, A.S.; Luco, N. A probabilistic seismic risk assessment procedure for nuclear power plants: (I) Methodology. *Nucl. Eng. Des.* **2011**, *241*, 3996–4003. [CrossRef]
64. Chaudhari, V.; Somala, S.N. Fragility of offshore wind turbines variation with pulse-period and amplitude: Directivity and Fling step. *Structures* **2022**, *41*, 66–76. [CrossRef]
65. Lee, S.-G.; Kim, D.-H.; Yoon, G.-L. Seismic Fragility for 5MW Offshore Wind Turbine using Pushover Analysis. *J. Ocean Eng. Technol.* **2013**, *27*, 98–106. [CrossRef]
66. Martìn del Campo, J.O.; Pozos-Estrada, A.; Pozos-Estrada, O. Development of fragility curves of land-based wind turbines with tuned mass dampers under cyclone and seismic loading. *Wind Energy* **2021**, *24*, 737–753. [CrossRef]
67. Mo, R.; Kang, H.; Li, M.; Zhao, X. Seismic Fragility Analysis of Monopile Offshore Wind Turbines under Different Operational Conditions. *Energies* **2017**, *10*, 1037. [CrossRef]
68. Wei, K.; Arwade, S.; Myers, A.; Hallowell, S.; Hajjar, J.; Hines, E. Performance Levels and Fragility for Offshore Wind Turbine Support Structures During Extreme Events. In Proceedings of the ASCE Structures Congress: 2015, Portland, OR, USA, 23–25 April 2015; pp. 1891–1902. [CrossRef]
69. Jeon, S.; Kim, B.; Huh, J. Comparison and verification of wake models in an onshore wind farm considering single wake condition of the 2 MW wind turbine. *Energy* **2015**, *93*, 1769–1777. [CrossRef]
70. Tavner, P. Offshore Wind Turbines: Reliability, Availability and Maintenance. The Institution of Engineering and Technology, IET: London, UK, 2012; ISBN 978-1-84919-229-3.
71. Fortes, P.; Alvarenga, A.; Seixas, J.; Rodrigues, S. Long-term energy scenarios: Bridging the gap between socio-economic storylines and energy modeling. *Technol. Forecast. Soc. Chang.* **2015**, *91*, 161–178. [CrossRef]
72. Shields, M.; Beiter, P.; Nunemaker, J. *A Systematic Framework for Projecting the Future Cost of Offshore Wind Energy*; National Renewable Energy Lab (NREL): Golden, CO, USA, 2022.
73. Schmitt, A.; Zhou, H. *EU Energy Outlook 2060*; Energy Brainpool: Berlin, Germany, 2022. Available online: https://blog.energybrainpool.com/en/eu-energy-outlook-2060-how-will-the-european-electricity-market-develop-over-the-next-37-years/ (accessed on 30 April 2025).
74. Burger, M.; Graeber, B.; Schindlmayr, G. *Managing Energy Risk*; John Wiley & Sons Ltd: Chichester, UK, 2014.
75. Bartlett, J. Reducing risk in merchant wind and solar projects through financial hedges. *Resour. Future* **2019**, *23*, 11–26.
76. Aydin, C.; Graves, F.; Villadsen, B. *Managing Price Risk for Merchant Renewable Investments: Role of Market Interactions and Dynamics on Effective Hedging Strategies*; The Brattle Group, 2017. Available online: https://www.brattle.com/wp-content/uploads/2017/10/7380_managing_price_risk_for_merchant_renewable_investments.pdf (accessed on 13 February 2025).
77. Mack, I.M. *Energy Trading and Risk Management: A Practical Approach to Hedging, Trading and Portfolio Diversification*; John Wiley and Sons: Hoboken, NJ, USA, 2014.
78. Härdle, W.K.; Cabrera, B.L.; Melzer, A. Pricing Wind Power Futures. *J. R. Stat. Soc. Ser. C Appl. Stat.* **2021**, *70*, 1083–1102. [CrossRef]
79. Huisman, R.; Koolen, D.; Stet, C. Pricing forward contracts in power markets with variable renewable energy sources. *Renew. Energy* **2021**, *180*, 1260–1265. [CrossRef]
80. Yamada, Y. Risk Management Tools for Wind Power Trades: Weather Derivatives on Forecast Errors. In *Handbook of Wind Power Systems*; Springer: Berlin/Heidelberg, Germany, 2014; pp. 39–66.
81. Dykes, K.; De Neufville, R. Real Options for a Wind Farm in Wapakoneta, Ohio: Incorporating Uncertainty into Economic Feasibility Studies for Community Wind. In Proceedings of the World Wind Energy Conference 2008, Kingston, ON, Canada, 24–26 June 2007. Available online: https://www.osti.gov/etdeweb/biblio/21095663 (accessed on 13 February 2025).
82. Bessembinder, H.; Lemmon, M.L. Equilibrium Pricing and Optimal Hedging in Electricity Forward Markets. *J. Finance* **2002**, *57*, 1347–1382. [CrossRef]
83. Jonkman, J.; Butterfield, S.; Musial, W.; Scott, G. *Definition of a 5-MW Reference WIND Turbine for Offshore System Development*; National Renewable Energy Lab (NREL): Golden, CO, USA, 2009.
84. Eurostat. Industrial Producer Price Index Overview. Available online: https://ec.europa.eu/eurostat/statistics-explained/index.php?title=Industrial_producer_price_index_overview (accessed on 13 February 2025).
85. Lecca, P.; McGregor, P.G.; Swales, K.J.; Tamba, M. The importance of learning for achieving the UK's targets for offshore wind. *Ecol. Econ.* **2017**, *135*, 259–268. [CrossRef]

86. Hancock, T.; Bezold, C. Possible futures, preferable futures. *Healthc. Forum J.* **1994**, *37*, 23–29.
87. Taylor, C.W. *Creating Strategic Visions*; Army War College, Strategic Studies Institute, Carlisle Barracks: Carlisle, PA, USA, 1990.
88. Voros, J. A generic foresight process framework. *Foresight* **2003**, *5*, 10–21. [CrossRef]
89. Voros, J. Big History and anticipation: Using Big History as a framework for global foresight. In *Handbook of Anticipation: Theoretical and Applied Aspects of the Use of Future in Decision Making*; Poli, R., Ed.; Springer: Berlin/Heidelberg, Germany, 2019; pp. 425–464.
90. Fingersh, L.; Hand, M.; Laxson, A. *Wind Turbine Design Cost and Scaling Model*; National Renewable Energy Lab (NREL): Golden, CO, USA, 2006.
91. Poore, R.; Lettenmaier, T. *Alternative Design Study Report: WindPACT Advanced Wind Turbine Drive Train Designs Study; November 1, 2000–February 28, 2002*; National Renewable Energy Lab (NREL): Golden, CO, USA, 2003.